

The electrostatics of Ta₂O₅ in Si-based metal oxide semiconductor devices

Lior Kornblum,^{1,a)} Boris Meyler,² Joseph Salzman,² and Moshe Eizenberg¹

¹*Department of Materials Science & Engineering, Technion—Israel Institute of Technology, Haifa 32000, Israel*

²*Department of Electrical Engineering, Technion—Israel Institute of Technology, Haifa 32000, Israel*

(Received 14 December 2012; accepted 6 February 2013; published online 20 February 2013)

Thin dielectric layers are a prominent route to control the band alignments and effective work function of metal oxide semiconductor (MOS) devices. In this work, the electrostatic effects of thin Ta₂O₅ layers on the band alignments of MOS devices are examined. A detailed analysis of the physical properties of a thick (~6 nm) Ta₂O₅ layer is reported. No significant dipoles at Ta₂O₅-Al₂O₃ and Ta₂O₅-SiO₂ interfaces are found, as well as any significant charges inside Ta₂O₅ layers. When positioned at the interface, Ta₂O₅ is shown to prevent the formation of band offsets between Al₂O₃-SiO₂, resulting in a shift of 1 ± 0.2 eV versus samples without interfacial Ta₂O₅. The relatively large magnitude of this shift in the current experimental configuration compared to previous works may indicate the participation of interface charges in the band offset. The possible use for these effects in devices is discussed. © 2013 American Institute of Physics.

[<http://dx.doi.org/10.1063/1.4792750>]

I. INTRODUCTION

High-*k* dielectrics with metal gates (HKMG) were introduced into the microelectronics industry several years ago, following a decade of intensive research on the relationship between the materials and the electrical properties of these materials and their interfaces.¹ Hf-based oxides emerged as the leading high-*k* dielectric.² An important aspect with the usage of HKMG in metal oxide semiconductor (MOS) technology is the position of the metal Fermi level with respect to the semiconductor, which can be described in terms of an effective work function³ (EFW). The EFW has a critical role in determining the performance of a single device and the entire circuit.⁴ Initially, controlling the EFW was attempted by engineering the metal gate by the use of alloys, which was shown to result in several metallurgical and thermal stability challenges.^{5–8}

Alternatively, it was shown that thin dielectrics layers, so called capping layers, placed at the metal-dielectric interface, can be useful for controlling the EFW.^{9,10} Typically, Al oxide is used for increasing the EFW^{11,12} and La oxide^{13–16} (and to some extent Gd oxide^{17,18}) for decreasing the EFW. It was shown that the position of the capping layers' atoms is important for their functionality,^{19,20} and particularly it was shown with different configurations that the contact of Al oxide with SiO₂ is responsible for the EFW increase.^{12,21,22} These effects have been further utilized recently for improving metal-semiconductor contacts.^{23,24}

In a recent study,²² we have shown that the formation of a Ta suboxide layer formed at a Ta-Al₂O₃ interface resulted in an EFW increase of 0.4 eV. Following this, in the current work, we studied the effect of deposited thin Ta₂O₅ layers in conjunction with Al₂O₃ on the electrical properties of MOS capacitors.

Despite its relatively large band gap, Al₂O₃ does not have a high enough *k* value to be used as a gate dielectric for

Si MOS devices. However, other than its use as a capping layer, Al₂O₃ is relevant for metal-insulator-metal (MIM) capacitors and for nonvolatile memories.²⁵ Moreover, Al₂O₃ is an important dielectric for MOS devices based on high-mobility semiconductors such as GaAs,²⁶ InGaAs,^{27,28} and Ge,²⁹ where it can be used in a bilayer configuration with another dielectric.^{30,33} Ta₂O₅ was among the first candidates in the early days of high-*k* dielectrics.^{4,34} However, it was abandoned as the main high-*k* dielectric for MOS devices, due to insufficient thermal stability and a too small conduction band offset with Si.¹

In order to understand the role of Ta₂O₅ on the band structure, Al₂O₃-based MOS devices were fabricated with varying positions of thin Ta₂O₅ layers. Since atomic layer deposition (ALD) of Ta₂O₅ is less robust than in the case of Al₂O₃, a physical characterization of ALD-Ta₂O₅ was carried out first.

II. EXPERIMENTAL

A 4.5 nm layer of SiO₂ was thermally grown on a (100) p-Si wafer (B doped, $\sim 2 \times 10^{15}$ cm⁻³). ALD of Al₂O₃ and Ta₂O₅ was performed at 300 °C using trimethyl-aluminum (TMA) and pentakis(dimethylamino)-tantalum^{31,32} (PDMAT) with H₂O, respectively. The different dielectric stacks are schematically shown in Fig. 1. Capacitors were formed by e-beam evaporation of 40 nm Pt through a shadow mask with a nominal contact area of 2.5×10^{-3} cm². The actual area was measured individually for each capacitor using an optical microscope. A back contact was formed by e-beam evaporation of 300 nm of Al. The samples were then annealed at 400 °C for 30 min at 10^{-7} Torr.

Capacitance-voltage (C-V) measurements were done with an HP4284A LCR meter in a light-sealed chamber at 100 KHz. Transmission electron microscopy (TEM) was done using an FEI Technai G² T20 microscope operated at 200 kV. X-ray photoelectron spectroscopy (XPS) measurements were done using a Thermo VG Scientific Sigma Probe

^{a)}liorkorn@gmail.com.

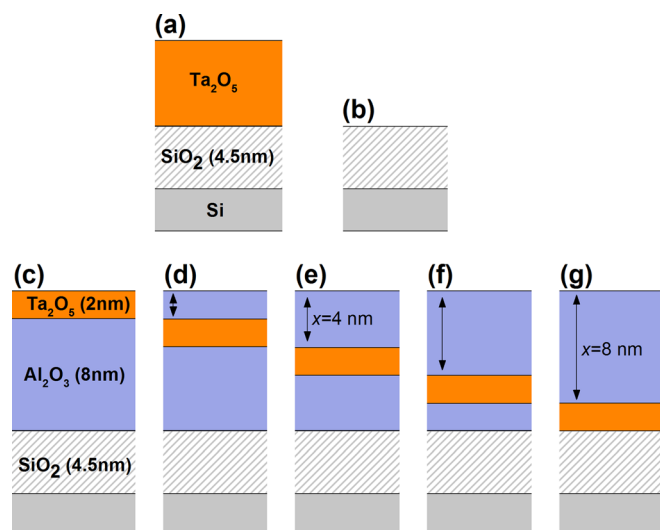


FIG. 1. Schematic cross section of the different samples, (a) thick Ta₂O₅ layer on SiO₂, (b) reference sample with no Ta₂O₅ (c)–(g) varying Ta₂O₅ position in a Al₂O₃ with $x = 0, 2, 4, 6,$ and 8 nm.

using a monochromatic Al K α (1486.7 eV) as a primary beam and pass energies of 20 and 50 eV for Ta 4f and O 1s, respectively. The energy scale was aligned by adjusting the C 1s peak of the adventitious carbon to 284.5 eV.

III. RESULTS AND DISCUSSION

A. Ta₂O₅ characterization

Ta₂O₅ deposition is not reported as extensively as that of Al₂O₃ in the literature and is more sensitive to process conditions due to lower precursor vapor pressure and reactivity. Therefore, the physical properties of a “thick” Ta₂O₅ layer were investigated prior to its application as a thin dielectric. A cross section TEM micrograph (Fig. 2(a)) shows a uniform and dense layer. A thickness of 4.5 ± 0.4 nm and 6.1 ± 0.7 nm for SiO₂ and Ta₂O₅, respectively, is obtained from Fig. 2(a), with the latter used for calibrating the thickness in the deposition of the subsequent samples.

Capacitance-voltage curves of the Ta₂O₅ are compared to those of the same device without the Ta₂O₅ layer (Fig. 2(b)). Leakage currents measured on sample b (with the smallest effective oxide thickness, EOT) were found to be below 10^{-7} A/cm² in the voltage range of Fig. 2(b). The Ta₂O₅ contribution to the capacitance, $C_{Ta_2O_5}$, can be calculated by $C_{Ta_2O_5}^{-1} = C_{(a)}^{-1} - C_{(b)}^{-1}$, with $C_{(a)}$, $C_{(b)}$ being the capacitance of samples a and b (Fig. 1) taken at accumulation (Fig. 2(b)). Using $C_{Ta_2O_5}$ and the measured Ta₂O₅ thickness (Fig. 2(a)), a dielectric constant of 22.3 ± 2.5 is calculated, with the error stemming from the uncertainty of the Ta₂O₅ thickness measurement. This value is in agreement with the earlier reports.^{1,34} The use of a bottom SiO₂ layer and the reference sample circumvents the deposition of the dielectric directly on Si, which usually forms a silicate interface layer (e.g., Refs. 32 and 35) that complicates the analysis and can lead to significant errors.

The Ta 4f XPS spectrum of the Ta₂O₅ layer shown in Fig. 2(c) displays a single doublet corresponding to fully oxidized Ta. No other components can be observed in the lower

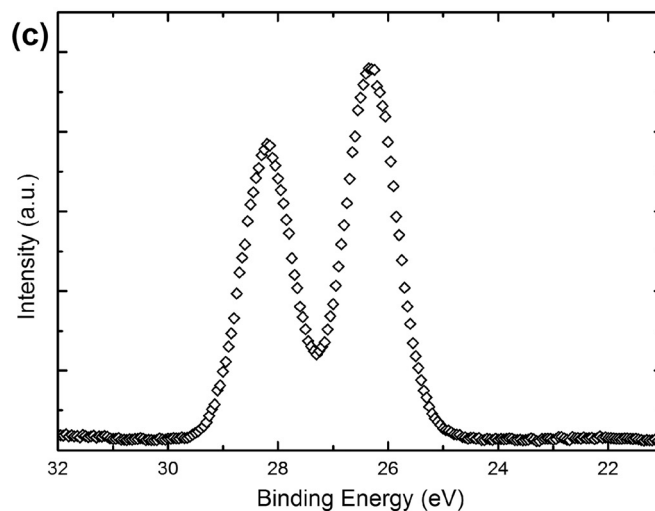
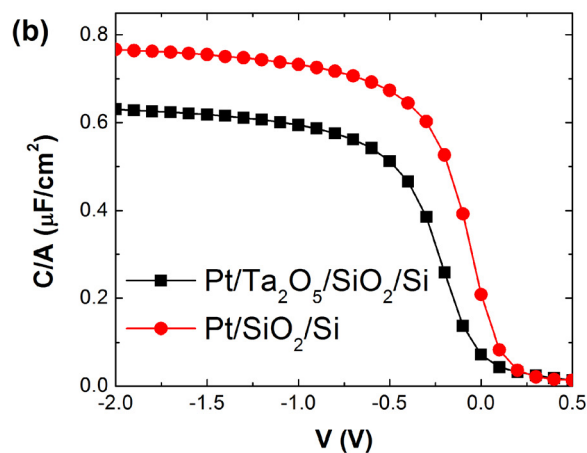
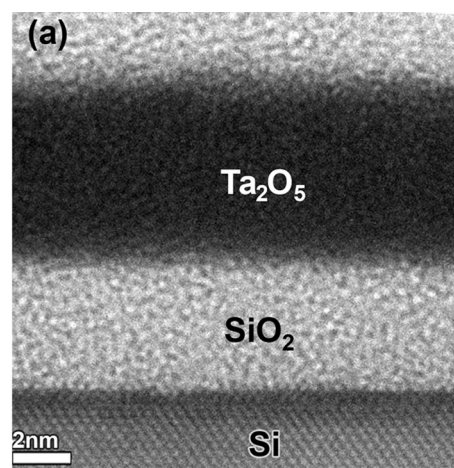


FIG. 2. (a) Cross section TEM micrograph of a 6.1 nm Ta₂O₅/4.5 nm SiO₂/Si stack. (b) Capacitance-voltage curves compared to a reference sample without Ta₂O₅. The lines connect the data points for clarity. (c) Ta 4f XPS spectrum.

binding energies^{22,36} indicating that up to the detection limit of XPS, the deposited layer is fully oxidized. It should be noted that the carbon content is not evaluated in this work due to the difficulties associated with quantifying carbon by XPS. A survey XPS scan reveals a 25 ~ 30% surface concentration of carbon which is typical of samples exposed to the atmosphere and cannot be used for actual quantification.

Given the agreement of the physical properties to previous reports, it is concluded that no abnormalities in the C content exist in the samples.

The O 1s XPS spectrum shown in Fig. 3 is fitted using a Shirley-type background, and peak parameters of 1.56 eV full width at half-maximum, and 12% Lorenzian-Gaussian ratio. The major component (“Peak1”) is attributed to O-Ta bonding states, while the minor components (“Peak2”, “Peak3”) can be attributed to small O-Si signal coming from the bottom SiO₂ layer and/or to surface contamination oxygen bonds.

The method used by Miyazaki *et al.*^{37,38} is applied for the extraction of the band gap of Ta₂O₅ by measuring the distance between the O-Ta component to the onset of the plasmon losses signal. The latter is obtained by the intersection of the linear fit of the plasmon losses slope with the background.^{39,40} This procedure results in a band gap value of 4.5 ± 0.2 eV, in agreement with the reported values of 4.4–4.65 eV (Refs. 1 and 38). Changes in the parameters of the peak fitting do not change the position of the major peak by more than 0.05 eV, which is much smaller than the estimated error in the band gap, attributed mostly to the plasmon-background intersection.

B. Ta₂O₅ in Al₂O₃-MOS devices

After asserting that the physical properties of Ta₂O₅ are well within the expected parameters, it is incorporated as a thin layer in Al₂O₃-based MOS capacitors by the preparation of the set of samples described in Fig. 1. A cross section TEM micrographs (Fig. 4) of a representative sample (corresponding to that of Fig. 1(g)) show that even for a Ta₂O₅ as thin as ~ 2 nm, it is continuous. In order to understand the electrostatic role of the Ta₂O₅ layer, a series of samples were produced in which the distance of the layer from the metal-dielectric interface, denoted x in Fig. 1, is varied from the top interface ($x = 0$ nm, Fig. 1(c)) to the bottom interface ($x = 8$ nm, Fig. 1(g)). It is expected that if Ta₂O₅ contains any significant charges, the flatband voltage (V_{FB}) of the

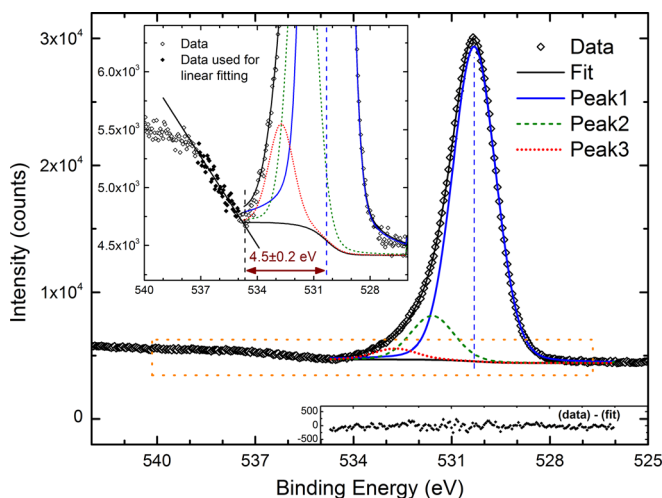


FIG. 3. O 1s XPS spectrum and its EELS tail; inset showing an enlargement of the dashed rectangle with the details of band gap extraction, bottom bar showing the fitting error.

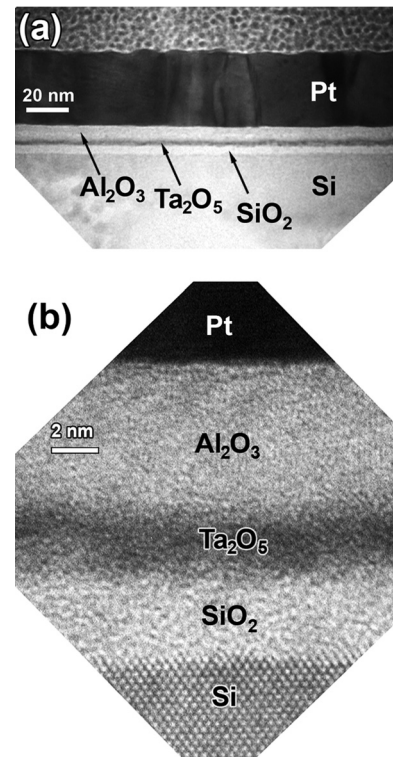


FIG. 4. Cross-section TEM micrograph of a $x = 8$ nm sample (Fig. 1(g)) at a low (a) and high (b) magnifications.

capacitors will change linearly with x .⁴¹ Alternatively, if dipoles are formed at Ta₂O₅-Al₂O₃ interfaces, they will cancel each other on both sides of the Ta₂O₅ layer for all samples except $x = 0$ and 8 nm.

The C-V characteristics of the Ta₂O₅-Al₂O₃ samples show well-behaved curves with a consistent accumulation capacitance (Fig. 5(a)). Interestingly, the V_{FB} values of all the samples are quite close (Fig. 5(b)), with the exception of the sample where the Ta₂O₅ layer is positioned at the Al₂O₃-SiO₂ interface ($x = 8$ nm, Fig. 1(g)).

The constant value of V_{FB} for $x = 0$ –6 nm rules out the existence of Ta₂O₅ (bulk or surface) charges that have any significance in terms of the C-V behavior of MOS devices. This is consistent with the behavior observed in Fig. 2(b). Next, dipoles at the Ta₂O₅-Al₂O₃ interface are considered; in the $x = 2$ –6 nm samples such dipoles would cancel each other from both sides of the Ta₂O₅ layer, having no net effect. However, no deviation of the C-V behavior occurs at the $x = 0$ nm sample, where there is only one Ta₂O₅-Al₂O₃ interface, indicating that no significant dipoles exist between these two materials. To complement and support this conclusion, we note that no significant differences are observed in (a) the V_{FB} of Pt/Ta₂O₅ versus Pt/SiO₂ (Fig. 2(b)) and (b) in the band alignment at Pt/Al₂O₃ interfaces versus Pt/SiO₂ (Ref. 22).

Examining the sample with $x = 8$ nm, we note that it consists of a Ta₂O₅-SiO₂ interface that shows no significant dipole (Fig. 2(b)), and an Al₂O₃-Ta₂O₅ interface that shows no dipole as well, as discussed in the previous paragraph. This means that the only electrostatic contribution of Ta₂O₅ at the Al₂O₃-SiO₂ interface is by creating a separation between Al₂O₃ and SiO₂. Indeed, it is known that an

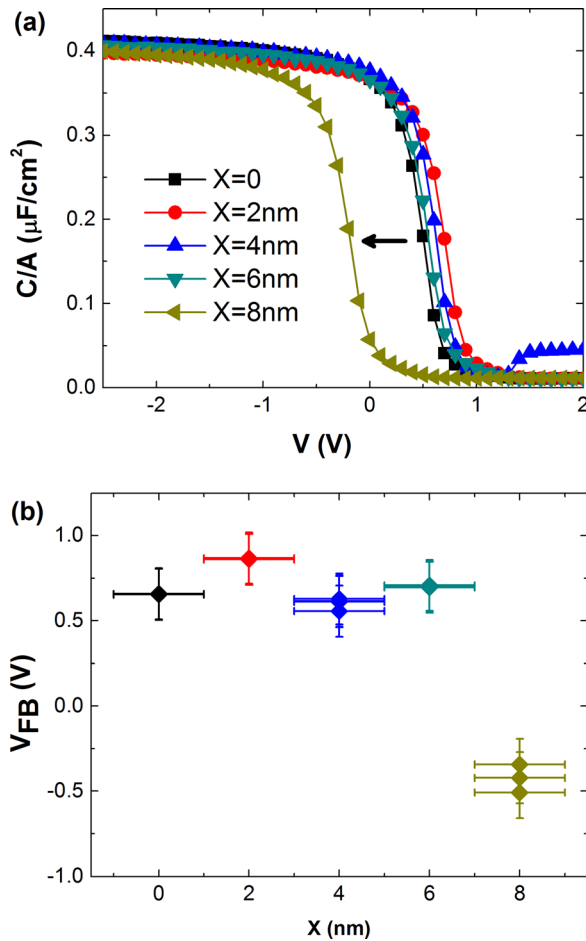


FIG. 5. (a) Capacitance-voltage curves of the Ta₂O₅-Al₂O₃ system and (b) the effect of the position of a Ta₂O₅ layer (x) on the flatband voltage.

Al₂O₃-SiO₂ contact increases the EWF (and V_{FB}), and we have previously reported an increase of 0.4 eV,^{12,22,42} in agreement with other reports of 0.2 ~ 0.7 eV.^{20,43-45} By contrast, in the current work, the contribution of the Al₂O₃-SiO₂ interface is 1 ± 0.2 eV (Fig. 5(b)). The principal difference between the current work and the literature is the larger EOT between the Al₂O₃-SiO₂ interface and the top metal, which is ~4 nm in the current work versus ~2 nm in previous reports.^{22,42} According to the Poisson equation,⁴¹ the potential shift caused by Al₂O₃-SiO₂ interface charges will have a distance (between the metal and the Al₂O₃-SiO₂ interface) dependence. If this V_{FB} shift indeed depends on the EOT of the Al₂O₃ layer, it could imply that charges at the Al₂O₃-SiO₂ interface may play a role in the shift, as argued before.⁴⁵

These results may seem to contradict those obtained with Ta(TaO_x)-Al₂O₃ interfaces, where a TaO_x layer was formed and shown to cause a surface dipole attributed to Ta-O bonds.²² However, the previous case is different from the Ta₂O₅-Al₂O₃ system in several aspects. The TaO_x layer was formed by a reaction between Al₂O₃ and Ta, resulting in a different metal-dielectric interface compared to the case of metal deposited on the dielectric in the current work. Moreover, the TaO_x layer was found to contain almost no fully oxidized Ta₂O₅ (mostly suboxide components), meaning that the chemical state of the interface layer is different.

Therefore, the structure and chemistry differences between TaO_x and Ta₂O₅ explain the difference in the electrical behavior.

IV. CONCLUSIONS

Ta₂O₅ can be grown by ALD to form thin and uniform layers having a high dielectric constant. Although not suitable as a single layer high-k dielectric,¹ the electrostatic inertness of thin Ta₂O₅ layers demonstrated in this work can be harnessed to several purposes. First, a thin Ta₂O₅ layer can be used to reduce and thereby control the dipole at Al₂O₃-SiO₂ interfaces. Moreover, the high dielectric constant of Ta₂O₅ allows flexibility in use, with a small EOT increase (~0.18 nm per 1 nm of physical thickness).

Al₂O₃ is emerging as the leading dielectric for the challenging surface passivation of high channel mobility MOS devices, but its relatively low dielectric constant compromises its scalability. The results of this work suggest a combination of Al₂O₃ and Ta₂O₅ as a possible route for this area as well.

The low conduction band offsets of Ta₂O₅ can be turned into an advantage when used as a charge trapping layer in non-volatile memories (NVMs).⁴⁶ Our results can further be applied for band structure engineering in such devices, keeping in mind that Al₂O₃ is a useful blocking layer in NVMs.²⁵

In summary, the properties of Ta₂O₅ films were studied electrically, structurally, and chemically. A systematic variation of the position of thin Ta₂O₅ layers inside Al₂O₃-based MOS devices has excluded the existence of significant charges inside the layer and dipoles at the Al₂O₃-Ta₂O₅ interface. Furthermore, it was shown that thin Ta₂O₅ can prevent the formation of the band offset that is known to exist at Al₂O₃-SiO₂ interfaces. The results further indicate the possibility that this offset may be partially caused by interface charges.

ACKNOWLEDGMENTS

This work was supported by the ALPHA consortium of the Israeli Ministry of Industry, Trade and Labor and by the Russell Berrie Nanotechnology Institute at the Technion. Sample preparation for this work was done with the support of the Technion's Micro-Nanoelectronic Fabrication Unit (MNFU). The authors thank Dr. Reuven Brenner for assistance with XPS measurements and analysis, Dr. T. Cohen-Hyams and Roy Winter for TEM samples preparation.

¹J. Robertson, *Rep. Prog. Phys.* **69**, 327 (2006).

²J. H. Choi, Y. Mao, and J. P. Chang, *Mater. Sci. Eng. R* **72**, 97 (2011).

³J. Robertson, *J. Vac. Sci. Technol. B* **27**, 277 (2009).

⁴G. D. Wilk, R. M. Wallace, and J. M. Anthony, *J. Appl. Phys.* **89**, 5243 (2001).

⁵J. Kwon and Y. J. Chabal, *J. Appl. Phys.* **107**, 123505 (2010).

⁶J. Avner Rothschild, A. Cohen, A. Brusilovsky, L. Kornblum, Y. Kauffmann, Y. Amouyal, and M. Eizenberg, *J. Appl. Phys.* **112**, 013717 (2012).

⁷L. Pantisano, T. Schram, Z. Li, J. G. Lisoni, G. Pourtois, S. De Gendt, D. P. Brunco, A. Akheyar, V. V. Afanas'ev, S. Shamuilia, and A. Stesmans, *Appl. Phys. Lett.* **88**, 243514 (2006).

⁸C. Cabral, C. Lavoie, A. S. Ozcan, R. S. Amos, V. Narayanan, E. P. Gusev, J. L. Jordan-Sweet, and J. M. E. Harper, *J. Electrochem. Soc.* **151**, F283 (2004).

- ⁹P. D. Kirsch, P. Sivasubramani, J. Huang, C. D. Young, M. A. Quevedo-Lopez, H. C. Wen, H. Alshareef, K. Choi, C. S. Park, K. Freeman, M. M. Hussain, G. Bersuker, H. R. Harris, P. Majhi, R. Choi, P. Lysaght, B. H. Lee, H. H. Tseng, R. Jammy, T. S. Böske, D. J. Lichtenwalner, J. S. Jur, and A. I. Kingon, *Appl. Phys. Lett.* **92**, 092901 (2008).
- ¹⁰A. Huang, X. Zheng, Z. Xiao, M. Wang, Z. Di, and P. K. Chu, *Chin. Sci. Bull.* **57**, 2872 (2012).
- ¹¹H. J. Li and M. I. Gardner, *IEEE Electron Device Lett.* **26**, 441 (2005).
- ¹²L. Kornblum, B. Meyler, C. Cytermann, S. Yofis, J. Salzman, and M. Eizenberg, *Appl. Phys. Lett.* **100**, 062907 (2012).
- ¹³H. N. Alshareef, M. Quevedo-Lopez, H. C. Wen, R. Harris, P. Kirsch, P. Majhi, B. H. Lee, R. Jammy, D. J. Lichtenwalner, J. S. Jur, and A. I. Kingon, *Appl. Phys. Lett.* **89**, 232103 (2006).
- ¹⁴S. Guha, V. K. Paruchuri, M. Copel, V. Narayanan, Y. Y. Wang, P. E. Batson, N. A. Bojarczuk, B. Linder, and B. Doris, *Appl. Phys. Lett.* **90**, 092902 (2007).
- ¹⁵M. Di, E. Bersch, R. D. Clark, S. Consiglio, G. J. Leusink, and A. C. Diebold, *J. Appl. Phys.* **108**, 114107 (2010).
- ¹⁶W. J. Maeng, W.-H. Kim, and H. Kim, *J. Appl. Phys.* **107**, 074109 (2010).
- ¹⁷H. B. Park, C. S. Park, C. Y. Kang, S.-C. Song, B. H. Lee, T.-Y. Jang, T. W. Kim, J. K. Jeong, and R. Choi, *Appl. Phys. Lett.* **95**, 192113 (2009).
- ¹⁸H. N. Alshareef, J. A. Caraveo-Frescas, and D. K. Cha, *Appl. Phys. Lett.* **97**, 202108 (2010).
- ¹⁹M. Copel, S. Guha, N. Bojarczuk, E. Cartier, V. Narayanan, and V. Paruchuri, *Appl. Phys. Lett.* **95**, 212903 (2009).
- ²⁰M. Bosman, Y. Zhang, C. K. Cheng, X. Li, X. Wu, K. L. Pey, C. T. Lin, Y. W. Chen, S. H. Hsu, and C. H. Hsu, *Appl. Phys. Lett.* **97**, 103504 (2010).
- ²¹L. Q. Zhu, N. Barrett, P. Jégou, F. Martin, C. Leroux, E. Martinez, H. Grampeix, O. Renault, and A. Chabli, *J. Appl. Phys.* **105**, 024102 (2009).
- ²²L. Kornblum, J. Rothschild, Y. Kauffmann, R. Brenner, and M. Eizenberg, *Phys. Rev. B* **84**, 155317 (2011).
- ²³B. E. Coss, W. Y. Loh, R. M. Wallace, J. Kim, P. Majhi, and R. Jammy, *Appl. Phys. Lett.* **95**, 222105 (2009).
- ²⁴J. Hu, A. Nainani, Y. Sun, K. C. Saraswat, and H. S. Philip Wong, *Appl. Phys. Lett.* **99**, 252104 (2011).
- ²⁵M. Lisiansky, A. Heiman, M. Kovler, A. Fenigstein, Y. Roizin, I. Levin, A. Gladkikh, M. Oksman, R. Edrei, A. Hoffman, Y. Shnieder, and T. Claasen, *Appl. Phys. Lett.* **89**, 153506 (2006).
- ²⁶Y. C. Chang, C. Merckling, J. Penaud, C. Y. Lu, W. E. Wang, J. Dekoster, M. Meuris, M. Caymax, M. Heyns, J. Kwo, and M. Hong, *Appl. Phys. Lett.* **97**, 112901 (2010).
- ²⁷C. Hinkle, E. Vogel, P. Ye, and R. Wallace, *Curr. Opin. Solid State Mater. Sci.* **15**, 188 (2011).
- ²⁸E. J. Kim, E. Chagarov, J. I. Cagnon, Y. Yuan, A. C. Kummel, P. M. Asbeck, S. Stemmer, K. C. Saraswat, and P. C. McIntyre, *J. Appl. Phys.* **106**, 124508 (2009).
- ²⁹S. Swaminathan, Y. Sun, P. Pianetta, and P. C. McIntyre, *J. Appl. Phys.* **110**, 094105 (2011).
- ³⁰S. Swaminathan, M. Shandalov, Y. Oshima, and P. C. McIntyre, *Appl. Phys. Lett.* **96**, 082904 (2010).
- ³¹W. J. Maeng and H. Kim, *Electrochem. Solid-State Lett.* **9**, G191 (2006).
- ³²W. J. Maeng, S. J. Lim, S. J. Kwon, and H. Kim, *Appl. Phys. Lett.* **90**, 062909 (2007).
- ³³J. Ahn, I. Geppert, M. Gunji, M. Holland, I. Thayne, M. Eizenberg, and P. C. McIntyre, *Appl. Phys. Lett.* **99**, 232902 (2011).
- ³⁴C. Chaneliere, J. Autran, R. Devine, and B. Balland, *Mater. Sci. Eng. R* **22**, 269 (1998).
- ³⁵J. Lu and Y. Kuo, *Appl. Phys. Lett.* **87**, 232906 (2005).
- ³⁶M. Khanuja, H. Sharma, B. R. Mehta, and S. M. Shivaprasad, *J. Electron Spectrosc. Relat. Phenom.* **169**, 41 (2009).
- ³⁷S. Miyazaki, *J. Vac. Sci. Technol. B* **19**, 2212 (2001).
- ³⁸S. Miyazaki, *Appl. Surf. Sci.* **190**, 66 (2002).
- ³⁹I. Geppert, E. Lipp, R. Brenner, S. Hung, and M. Eizenberg, *J. Appl. Phys.* **107**, 053701 (2010).
- ⁴⁰P. Shekhter, L. Kornblum, Z. Liu, S. Cui, T. P. Ma, and M. Eizenberg, *Appl. Phys. Lett.* **99**, 232103 (2011).
- ⁴¹E. H. Nicollian and J. R. Brews, *MOS (metal oxide semiconductor) Physics and Technology* (Wiley, New York, 1982), Chap. 10, pp. 423–491.
- ⁴²L. Kornblum, P. Shekhter, Y. Slovatzky, Y. Amouyal, and M. Eizenberg, *Phys. Rev. B* **86**, 125305 (2012).
- ⁴³Y. Kamimuta, K. Iwamoto, Y. Nunoshige, A. Hirano, W. Mizubayashi, Y. Watanabe, S. Migita, A. Ogawa, H. Ota, and T. Nabatame, in *Proceedings of the Tech. Digest IEDM* (IEEE, Washington DC, 2007), p. 342.
- ⁴⁴K. Iwamoto, H. Ito, Y. Kamimuta, Y. Watanabe, W. Mizubayashi, S. Migita, Y. Morita, M. Takahashi, H. Ota, T. Nabatame, and A. Toriumi, in *Proceedings of the Symposium on VLSI Tech. Digest* (IEEE, Kyoto, Japan, 2007), p. 70.
- ⁴⁵J. A. Caraveo-Frescas, H. Wang, U. Schwingenschlögl, and H. N. Alshareef, *Appl. Phys. Lett.* **101**, 112902 (2012).
- ⁴⁶X. Wang, J. Liu, W. Bai, and D. L. Kwong, *IEEE Electron Device Lett.* **51**, 597 (2004).